



# Stabilization of GTSE1 by cyclin D1-CDK4/6 promotes cell proliferation: relevance in cancer prognosis

Reviewed Preprint


v1 • September 20, 2024

Not revised

Nelson García-Vázquez, Tania J González-Robles, Ethan Lane, Daria Spasskaya, Qingyue Zhang, Marc Kerzhnerman, YeonTae Jeong, Marta Collu, Daniele Simoneschi, Kelly V Ruggles, Gergely Rona, Michele Pagano , Sharon Kaisari 

Department of Biochemistry and Molecular Pharmacology, New York University Grossman School of Medicine, NYC, NY, USA • Department of Medicine, New York University Grossman School of Medicine, NYC, NY, USA • Howard Hughes Medical Institute, New York University Grossman School of Medicine, NYC, NY, USA • Institute of Molecular Life Sciences, HUN-REN Research Centre of Natural Sciences, Budapest, Hungary

 [https://en.wikipedia.org/wiki/Open\\_access](https://en.wikipedia.org/wiki/Open_access)

 Copyright information

## Abstract

Cyclin D1 is the activating subunit of the cell cycle kinases CDK4 and CDK6, and its dysregulation is a well-known oncogenic driver in many human cancers. The biological function of cyclin D1 has been primarily studied by focusing on the phosphorylation of the retinoblastoma (RB) gene product. Here, using an integrative approach combining bioinformatic analyses and biochemical experiments, we show that GTSE1 (G2 and S phases expressed protein 1), a protein positively regulating cell cycle progression, is a previously unknown substrate of cyclin D1-CDK4/6. The phosphorylation of GTSE1 mediated by cyclin D1-CDK4/6 inhibits GTSE1 degradation, leading to high levels of GTSE1 also during the G1 phase of the cell cycle. Functionally, the phosphorylation of GTSE1 promotes cellular proliferation and is associated with poor prognosis within a pan-cancer cohort. Our findings provide insights into cyclin D1's role in cell cycle control and oncogenesis beyond RB phosphorylation.

### eLife assessment

In this **valuable** study, García-Vázquez et al. provide **solid** evidence suggesting that G2 and S phases expressed protein 1 (GTSE1), is a previously unappreciated non-pocket substrate of cyclin D1-CDK4/6 kinases. To this end, this study holds a promise to significantly contribute to an improved understanding of the mechanisms underpinning cell cycle progression. Notwithstanding these clear strengths of the article, it was thought that the study may benefit from establishing the precise role of cyclin D1-CDK4/6 kinase-dependent GTSE1 phosphorylation in the context of cell cycle progression, obtaining more direct evidence that cyclin D1-CDK4/6 kinase phosphorylate indicated sites on GTSE1 (e.g., S454) and mapping a degron in GTSE1 whose function may be blocked by cyclin D1-CDK4/6 kinase-dependent phosphorylation.

<https://doi.org/10.7554/eLife.101075.1.sa4>

## Introduction

D-type cyclins (cyclin D1, cyclin D2 and cyclin D3) are activators of the cyclin-dependent kinases CDK4 and CDK6 and represent major oncogenic drivers among members of the cyclin superfamily<sup>1–4</sup>. The *CCND1* gene –encoding cyclin D1– shows some of the highest frequency of amplification and overexpression among cancer genes across a broad spectrum of human tumors<sup>5–9</sup>. Moreover, mutations in *CCND1*, which prevent the degradation of cyclin D1 by AMBRA1, a substrate receptor (SR) of a CUL4-RING ubiquitin ligase (CRL4) complex that targets all three D-type cyclins for proteasome-mediated degradation, have been reported in a variety of tumor types<sup>10–12</sup>. Deregulation of cellular proliferation, often mediated by uncontrolled CDKs' activation lies at the heart of cancer as a pathological process<sup>13</sup>.

The biological roles of D-type cyclins have been examined almost exclusively through the lens of E2F transcription regulation upon phosphorylation of the three pocket proteins, RB, p107, and p130. D type cyclins-mediated phosphorylation of RB results in the inactivation of its tumor suppressive effect by releasing E2F from the RB's inhibitory effect on gene transcription. Although the regulation of RB by phosphorylation is well understood in both physiology and human tumorigenesis, the role of phosphorylation of other substrates is a subject that has remained understudied. In this study, we characterize GTSE1 (G-Two and S-phase expressed protein 1) as a previously unidentified substrate of cyclin D1-CDK4/6. GTSE1 is a cell cycle-related protein expressed specifically during the S and G2 phases of the cell cycle<sup>14</sup>. It interacts with the tumor suppressor p53, and it induces its MDM2-mediated degradation in G2 and during the recovery from DNA damage, promoting cell proliferation<sup>14–18</sup>. Moreover, GTSE1 associates with growing microtubules, promoting cell migration<sup>19,20</sup>. In prometaphase, GTSE1 becomes highly phosphorylated by CDK1-cyclin B1, resulting in its recruitment to the inner spindle<sup>21</sup>. After anaphase, its dephosphorylation is followed by marked reduction in its abundance in G1<sup>18,22</sup>. Our findings demonstrate that the cyclin D1-CDK4/6-mediated phosphorylation of GTSE1 leads to its increased stability in G1 phase, an event that significantly impacts cell proliferation and cancer prognosis.

## Results and discussion

AMBRA1 is a substrate receptor of a CUL4-RING ubiquitin ligase (CRL4) complex that targets all three D-type cyclins for proteasome-mediated degradation<sup>10,11</sup>. To unveil new substrates of the cyclin D1-CDK4 complex, we performed a comprehensive multi-analysis of published data (Figure supplement 1A). First, we incorporated recent mass spectrometry data that compared the whole proteome of AMBRA1 knockout (KO) clones to parental U2OS cells<sup>11</sup>, aiming to pinpoint the top 30 proteins whose levels were elevated in the absence of AMBRA1, the SR of the ubiquitin ligase targeting D-type cyclins (Figure 1A). Subsequently, we asked which of these 30 proteins contain a canonical CDK phosphorylation consensus motif [S/T\*]PX[K/R], relying on the PhosphoSitePlus database<sup>23</sup> (Figure 1B). Finally, this dataset was integrated with findings from a proteomic screen assessing protein abundance fluctuations in the presence or absence of the CDK4/6 inhibitor, Palbociclib (Figure 1C)<sup>11</sup>. In summary, our analysis aimed at identifying proteins whose upregulation in AMBRA1 KO cells was counteracted by Palbociclib treatment, thereby filtering for proteins whose augmented abundance is attributed to CDK4/6-mediated phosphorylation events. GTSE1, a cell cycle-regulated protein expressed mainly during the G2 and S phases of the cell cycle<sup>14</sup>, emerged as the top hit in these orthogonal analyses. In mitosis GTSE1 is phosphorylated by CDK1-cyclin B1<sup>21</sup>, but its dephosphorylation at the end of mitosis is followed by marked reduction in its abundance, which remains low during the next G1<sup>18,22</sup>.

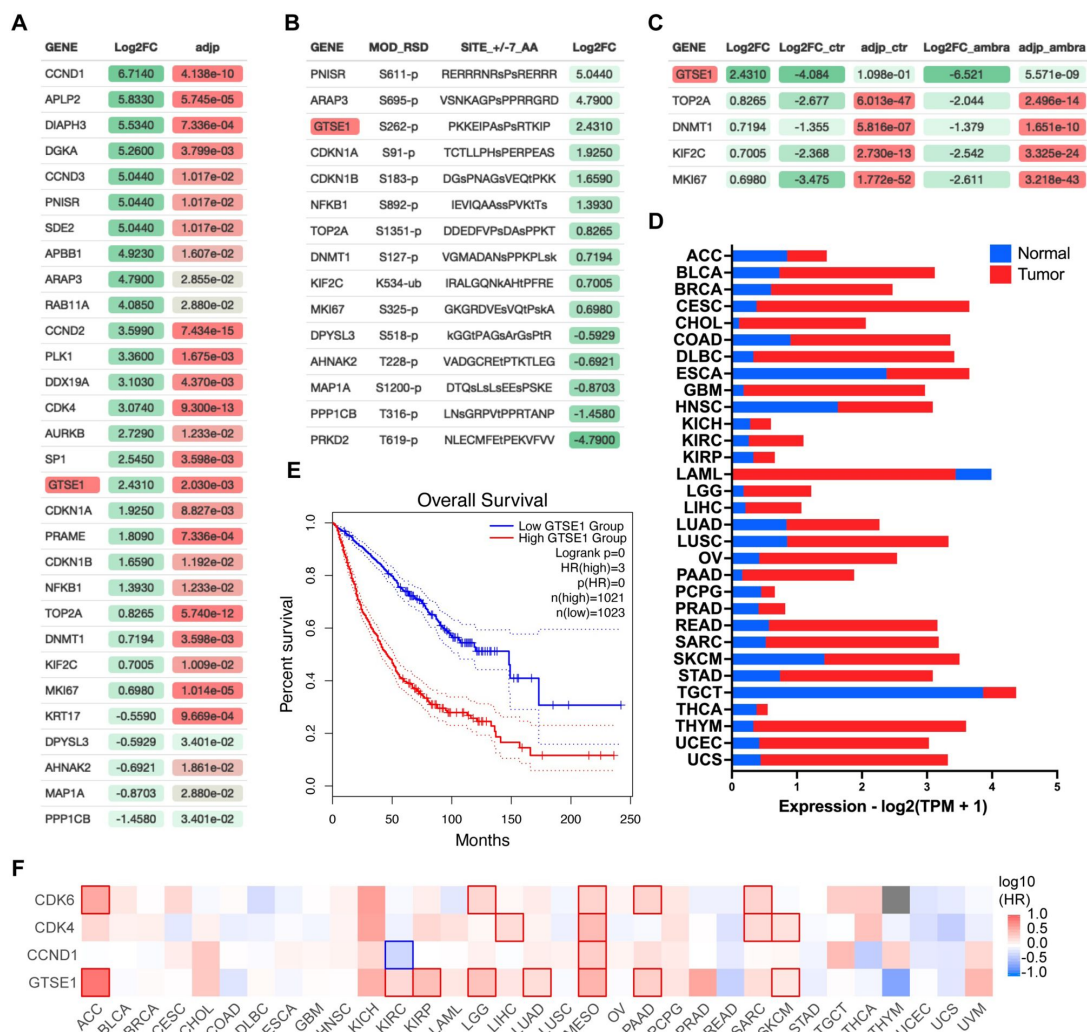


**Figure 1**

## Identification of GTSE1 as a cyclin D1-CDK4 substrate with prognostic significance in cancer

A) Differential proteomic profiling of AMBRA1 KO U2OS cells compared to parental U2OS cells<sup>11</sup>. Proteins with adjusted p value<0.05 were ranked by the log2 fold change (Log2FC) to quantify expression changes between AMBRA1 KO and parental cells. The top 30 upregulated proteins in this analysis are presented. Statistical significance was assessed by False Discovery Rate (FDR).

B) Subset of proteins from (A) containing a canonical CDK phosphorylation consensus motif [S/T\*]PX[K/R]. Annotated list of phosphorylated proteins was generated using PhosphoSitePlus database<sup>23</sup>.

C) Subset of proteins from (B) whose abundance was reverted to basal levels following treatment of AMBRA1 KO U2OS cells with Palbociclib<sup>11</sup> (Log2FC\_ambra) with adjusted p-values (adjp\_ambra)<0.001 were ranked by log2 fold change (Log2FC) from the original shotgun proteomic analysis (A) to integrate expression changes between AMBRA1 KO and parental cells under Palbociclib-treated versus untreated condition.

D) Transcriptomic analysis of GTSE1 in various cancer types, contrasting tumor (red) and normal tissue (blue) expression levels, using data derived from The Cancer Genome Atlas (TCGA)<sup>37</sup>. Statistical significance assessed by FDR, p<0.05.

E) Kaplan-Meier curves representing the overall survival analysis based on the 50% upper versus lower expression levels of GTSE1. Survival analysis was conducted across various cancer cohorts, including ACC, KIRC, KIRP, LGG, LUAD, MESO, PAAD, and SKCM (see also Figure supplement 1). The hazard ratio (HR) was calculated to estimate the relative risk, and significance was assessed using the log-rank test with a threshold of p<0.05. Curves were generated using the GEPIA2 platform.<sup>38</sup>

F) Survival map of various cancer types according to the indicated gene expression levels (50% upper and lower expression). Color intensity indicates the log of the HR, with red and blue representing poorer and better survival, respectively. Statistically significant differences in survival are denoted by highlighted contour squares, based on the log-rank test. Generated with GEPIA2 platform<sup>38</sup>, using TCGA data.

Recent pan-cancer analysis revealed that the expression of GTSE1 positively correlates with tumor mutational burden and microsatellite instability in most cancer types<sup>24</sup>. Specifically, high expression of GTSE1 was found to promote the proliferation and invasion of breast cancer cells<sup>25</sup>, and was associated with poor clinical prognosis in clear cell renal cell carcinoma<sup>26</sup>. We explored further the potential influence of GTSE1 on cancer prognosis and found that within multiple cancer cohorts, its elevated expression levels were correlated with a statistically significant poorer prognosis compared to lower expression levels (**Figure 1E**, Figure supplement 1B). This is noteworthy, since, except for acute myeloid leukemia (LAML), GTSE1 expression was higher than that in normal tissue counterparts in all tumor types analyzed (**Figure 1D**). We also assessed the impact of GTSE1 on survival across various cancer types (**Figure 1F**, Figure supplement 1B). For context, we compared the survival patterns associated with cyclin D1, CDK4, and CDK6. GTSE1 was found prognostically unfavorable across multiple cancer types, presenting a survival pattern similar to that of the cyclin D1-CDK4/6 gene cluster. In **Figure 1F**, those cancers in which differences in survival are statistically significant were denoted by contour squares.

Next, we sought to experimentally validate GTSE1 as a putative phosphorylation target of cyclin D1-CDK4. As a first step, we employed transient transfection to introduce in HEK293T various Flag-tagged constructs in the presence or absence of cyclin D1 and CDK4. GTSE1 showed an upper shift in a phos-tag<sup>TM</sup> gel when co-expressed with cyclin D1-CDK4, similar to the known substrates p107 and p130 (**Figure 2A**). In fact, a slight delay in GTSE1 migration is appreciable even in a regular SDS-PAGE (**Figure 2A**). The upper shift was not observed in ZC3HAV1, a protein used as negative control. Next, we performed an *in vitro* phosphorylation assay to directly assess the specificity of GTSE1 phosphorylation by cyclin D1-CDK4. Using purified, recombinant proteins, we subjected GTSE1 to a phosphorylation reaction with cyclin D1-CDK4 and analyzed the products using phos-tag<sup>TM</sup> gels. The results confirmed that GTSE1 underwent phosphorylation by cyclin D1-CDK4, but not by ERK1, another Pro-directed kinase (**Figure 2B**). Moreover, the phosphorylation was abolished in the presence of Palbociclib, similar to the pattern observed with RB (**Figure 2B,C**). Then, we asked whether GTSE1 physically interacts with the kinase complex. Overexpression of Flag-tagged cyclin D1 and CDK4 in HEK293T followed by a Flag pull-down demonstrated binding to endogenous GTSE1, similar to the canonical substrate RB (**Figure 2D**).

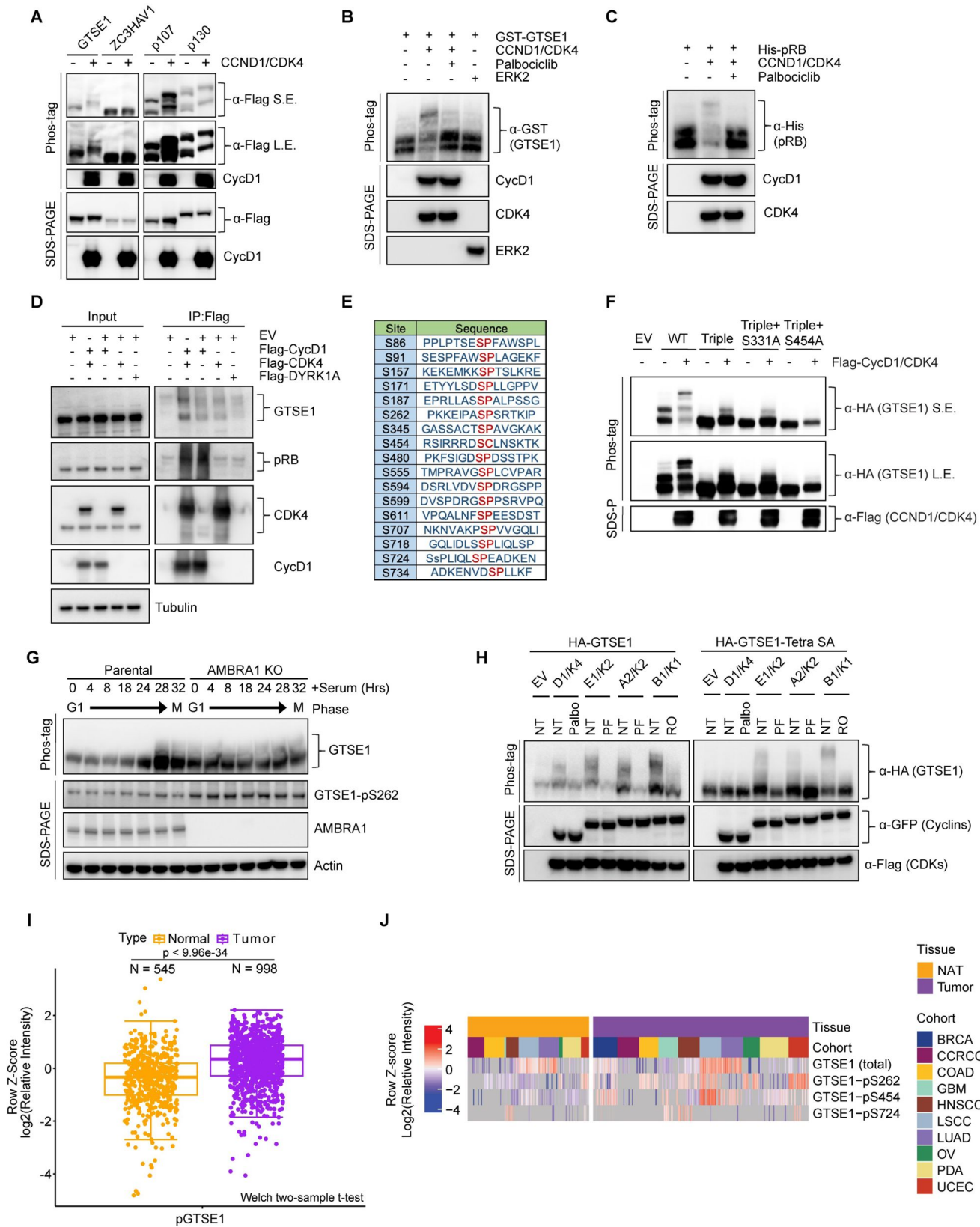


## Figure 2

### Cyclin D1-CDK4 promotes GTSE1 phosphorylation on four serine residues.

A) Immunoblot analysis following transient transfection of the indicated proteins in HEK293T cells detailing their phosphorylation status via differential mobility in phos-tag<sup>TM</sup> gels in the presence or absence of Cyclin D1-CDK4 co-expression.

B-C) The indicated purified, recombinant proteins were incubated in the presence or absence of recombinant cyclin D1-CDK4 complex. ERK2 was used as a negative control. Post-incubation, differential phosphorylation was analyzed using phos-tag<sup>TM</sup> gels to detect mobility shifts. Immunoblot analysis was conducted to verify the presence of the recombinant proteins as indicated.

D) HEK293T cells transfected with either the indicated Flag-tagged proteins or an empty vector (EV). Cell lysates were subjected to immunoprecipitation followed by immunoblot analysis. Inputs (5%) represent whole cell extracts before pull down.

E) Schematic representation of candidate CDK phosphorylation sites in GTSE1, as indicated by the PhosphoSitePlus database<sup>23</sup>.

F) HEK293T cells were transiently transfected with the indicated HA-GTSE1 mutants, in the presence or absence of Cyclin D1-CDK4 co-expression. Changes in protein migration were analyzed by phos-tag<sup>TM</sup> gels.

G) Immunoblot and phos-tag<sup>TM</sup> gel analysis displaying cell cycle synchronization effects following 72 hours of serum starvation in parental T98G cells and AMBRA1 KO T98G cells. Cells were collected at various time points post-serum re-supplementation as indicated, followed by immunoblotting with the indicated antibodies.

H) HA-tagged wild type GTSE1 (left) or GTSE1 mutated at positions 91, 261, 454, and 724 ('Tetra SA') (right) was subjected to co-expression with various cyclins and CDKs, in the presence or absence of the indicated kinase inhibitors to observe the impact on phosphorylation.

I) Boxplot representation of the log2-transformed Z-scores for bulk phospho-peptide abundance of GTSE1 across a pan-cancer cohort relative to adjacent normal tissue, utilizing data from the Clinical Proteomic Tumor Analysis Consortium (CPTAC)<sup>39</sup>. Statistical significance was assessed using the Wilcoxon rank-sum test, with a p-value threshold of <0.05.

J) Heatmap illustrating differential abundance in cancer of the three GTSE1 phosphorylation sites found in the current study using CPTAC data<sup>39</sup>. Color intensity reflects the log2-transformed Z-scores of identified GTSE1 phosphopeptides, indicating relative phosphorylation levels across various tumor cohorts compared to adjacent normal tissues. The complete analysis of all phosphorylation sites can be found in Figure supplement 3D.

Following these validation steps, we aimed at pinpointing the serine residue(s) modified by cyclin D1-CDK4. First, we generated a GTSE1 mutant in which Ser262 (see **Figure 1B**) was mutated to Ala. Since GTSE1 has additional, conserved serine residues followed by prolines, which could be potential CDK phosphorylation sites (**Figure 2E**, Figure supplement 2B), we also generated another 16 Ser-to-Ala GTSE1 mutants, and expressed them in HEK293T cell in the presence or absence of cyclin D1-CDK4 (Figure supplement 3A). When compared to wild-type GTSE1, two mutants displayed changes in their migrations on phos-tag<sup>TM</sup> gels (Figure supplement 3A), suggesting that Ser residues at positions 91 and 724 are sites potentially phosphorylated by cyclin D1-CDK4. PhosphoSitePlus<sup>23</sup> reports several high-throughput studies that, in addition to Ser262, identified phosphorylation also at Ser91 and Ser724, supporting our results. To corroborate the loss of cyclin D1-CDK4-dependent phosphorylation at these sites, we constructed a triple mutant

(S91A/S262A/S724A). This mutant displayed loss of slower-migrating bands relative to wild-type GTSE1, suggesting diminished phosphorylation (**Figure 2F**). Nevertheless, a residual slow-migrating band persisted, prompting further mutations of the triple GTSE1 mutant in two additional GTSE1 sites (individually), which do not have a CDK-phosphorylation consensus, but were identified in several proteomics studies<sup>23,27</sup>. From these two mutants, only the S454A mutation demonstrated a complete abrogation of any shift in phos-tag<sup>TM</sup> gels (**Figure 2F**). In contrast, a single S454A mutation showed only a minor effect on GTSE1 shift (data not shown). These studies suggest that four major sites (S91, S262, S454, and S724) are phosphorylated (either directly and/or indirectly) in a cyclin D1-CDK4-dependent manner.

To gain an insight into the cell-cycle pattern of GTSE1 abundance and phosphorylation status, we synchronized T98G cells (both parental and AMBRA1 knockout [KO] pooled clones) by serum starvation followed by serum re-addition. Parental cells displayed a fluctuation in GTSE1 abundance, with low levels in G1 that subsequently increased in S and G2 phases (Figure supplement 3B), in accordance with the literature<sup>18,22</sup>. In contrast, in AMBRA1 KO cells, GTSE1 levels were consistently elevated throughout the cell cycle, suggesting that elevated cyclin D1 levels are associated with an increased abundance of GTSE1 (Figure supplement 3B). Additionally, while phosphorylation of GTSE1 in the parental cell line peaked during the G2-M transition, AMBRA1 KO cells exhibited sustained phosphorylation of GTSE1 across all cell cycle phases (**Figure 2G**, Figure supplement 3B). We also generated a phospho-specific antibody that recognized GTSE1 only when phosphorylated on Ser262 (Figure supplement 3C). Using this antibody, we confirmed the data obtained with phos-tag<sup>TM</sup> gel indicating that in AMBRA1 KO cells, GTSE1 is hyper-phosphorylated (**Figure 2G**).

Next, we leveraged data from the Clinical Proteomic Tumor Analysis Consortium (CPTAC) to examine the relevance of the identified phosphorylation events in a clinical context. We observed an enrichment of GTSE1 phospho-peptides within a pan-cancer cohort as opposed to adjacent, corresponding normal tissues (**Figure 2I**), underscoring the potential role of GTSE1 phosphorylation in tumorigenesis. Upon analyzing single phosphorylated sites, we found that nine were statistically enriched in cancers. Of these, three sites (S262, S454, and S724) were identified as dependent on cyclin D1-CDK4 in our study (**Figure 2J** and Figure supplement 3D). (Data on Ser91 are not present in CPTAC.) These results underscore the potential pathophysiological significance of GTSE1 phosphorylation by cyclin D1-CDK4 in cancer.

Considering GTSE1 being an established target of cyclin B1-CDK1 during mitosis<sup>21</sup>, we aimed to elucidate the phosphorylation patterns of GTSE1 by various cyclin-CDK complexes operating at distinct cell cycle phases. Wild-type GTSE1 was found to be phosphorylated in HEK293T cells upon overexpression of all cyclin-CDK pairs, with its shifts in phos-tag<sup>TM</sup> gels being abolished upon treatment with the corresponding specific CDK inhibitor (**Figure 2H**, left panel). However, when the quadruple (S91A/S262A/S454A/S724A) GTSE1 mutant, referred to as “Tetra SA”, was expressed in HEK293T cells, cyclin D1-CDK4 was unable to induce any shift, whereas the other three cyclin-CDK pairs still sustained phosphorylation (**Figure 2H**, right panel). This suggests a unique phosphorylation profile conferred by cyclin D1-CDK4 in GTSE1, distinct from that induced by other cyclin-CDK complexes.

We noticed an elevation in endogenous GTSE1 levels in AMBRA1 knockout cells compared to the parental line (Figure supplement 3B and **Figure 3A**) in agreement with the findings of the proteomic screen performed in AMBRA1 KO cells<sup>11</sup> (**Figure 1B**). A similar increase was observed when overexpressing wild-type cyclin D1 and, even more, an AMBRA1-insensitive, stable mutant of cyclin D1 (T286A)<sup>10</sup> (**Figure 3A,B**), suggesting that the elevated GTSE1 levels are due to high D-type cyclins present in AMBRA1 knockout cells. We also used HCT116 cells harboring an endogenous fusion of AMBRA1 to a minimally constructed Auxin Inducible Degron (mAID) at the N-terminus<sup>28</sup>. This system allows for rapid and inducible degradation of AMBRA1 upon addition of auxin, thereby minimizing compensatory cellular rewiring. Again, we observed an increase in

GTSE1 levels upon acute ablation of AMBRA1 (*i.e.*, in 8 hours) (**Figure 3B** [↗](#)). In all cases, the upregulation in GTSE1 abundance was rescued upon Palbociclib treatment (**Figure 3A,B** [↗](#)), suggesting that this event was a consequence of increased levels of D-type cyclins. We also conducted cycloheximide chase assays in HCT-116 mAID-AMBRA1 cells to assess GTSE1 protein stability and degradation kinetics. The assays revealed that in the context of AMBRA1 depletion, GTSE1 exhibited a prolonged half-life and reduced degradation rate when compared to control cells (**Figure 3C** [↗](#)). A parallel half-life assessment in parental U2OS cells and two AMBRA1 knockout U2OS clones corroborated the finding that GTSE1 is stabilized in the absence of AMBRA1 (**Figure 3D** [↗](#)).

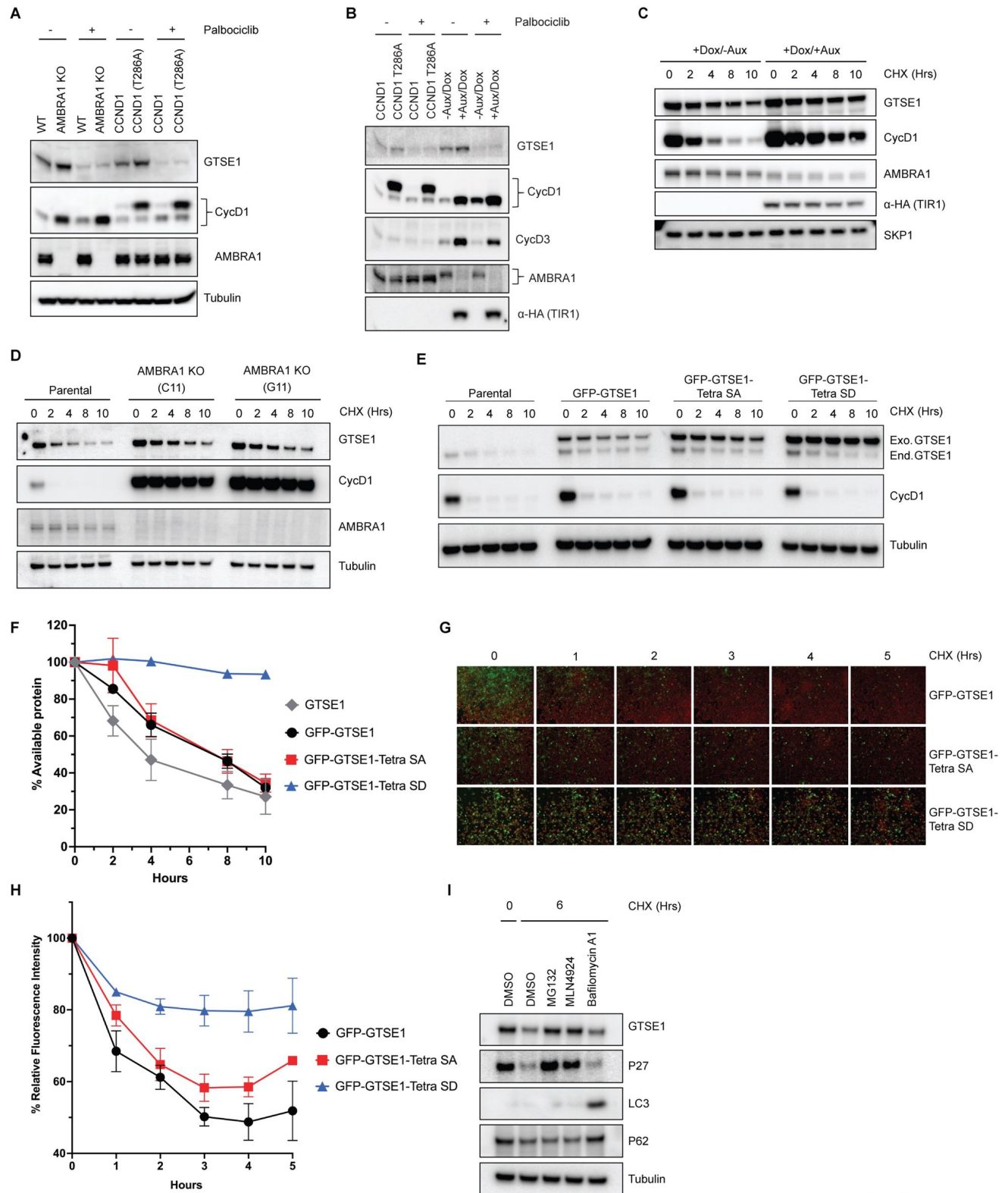


### Figure 3

#### GTSE1 protein is stabilized upon its phosphorylation by cyclin D1-CDK4

A) Immunoblot analysis of whole cell extracts from parental HCT-116 cells, AMBRA1 KO HCT-116 cells, and HCT-116 cells expressing either wild-type cyclin D1 or an AMBRA1-insensitive mutant of Cyclin D1 (T286A), in the presence or absence of the CDK4/6 inhibitor palbociclib.

B) Immunoblot analysis of whole cell extracts from HCT-116 cells harboring an endogenous mini-AID domain fused to AMBRA1 N-terminus. Cells were subjected to either incubation with auxin and doxycycline to induce AMBRA1 degradation or transfection with cyclin D1(T286A) in the presence or absence of Palbociclib.

C) Cycloheximide (CHX) chase assay in HCT116 cells with mAID-AMBRA1, treated with or without auxin and doxycycline to induce AMBRA1 degradation. Immunoblot analyses were conducted to assess the stability of GTSE1 and other indicated proteins, with the stable protein SKP1 used as a loading control.

D) Protein stability assessment via CHX chase in U2OS parental cells and AMBRA1 knockout clones (C11 and G11). The protein levels of AMBRA1, GTSE1, and cyclin D1 were analyzed by immunoblotting, with tubulin serving as a loading control.

E) U2OS cells stably transduced with retroviruses expressing the indicated GTSE1 constructs were subjected to cycloheximide CHX chase assays. Subsequent immunoblotting was conducted for the indicated proteins, with tubulin utilized as a loading control.

F) Densitometric quantification of GTSE1 band intensity from (E) and two identical experiments normalized using tubulin. Initial band intensity at time 0 is set as the 100% reference point. Error bars represent SEM (n=3 of biological replicates).

G) Time-lapse microscopy images of U2OS cells stably expressing EGFP-tagged the indicated GTSE1 constructs during a CHX chase. The EGFP signal intensity corresponds to GTSE1 levels, while cells are stained with a far-red cell tracker for cell masking.

H) Quantitative analysis of EGFP fluorescence intensity from time-lapse experiment shown in (G) plus two identical experiments. The initial fluorescence intensity was normalized to 100% at time zero. Data represent the mean fluorescence intensity from the three independent measurements, with error bars indicating the standard error of the mean (SEM).

I) U2OS cells were treated with various inhibitors for 3 hours before harvest: the proteasome inhibitor MG132, the CRL inhibitor MLN4924, and the V-ATPase inhibitor Bafilomycin A1. Immunoblot analysis of the indicated proteins was performed, with tubulin as a loading control. p62 and LC3 serve as autophagy inhibition controls, while p27 is used as control for CRL- and UPS-dependent degradation.

To further dissect the impact of cyclin D1-CDK4-mediated phosphorylation on GTSE1 stability, we engineered a phospho-mimicking mutant, referred to as “Tetra SD” with the 4 serine residues replaced with an aspartate at positions 91, 261, 454, and 724. To circumvent the variability of transient transfection, U2OS cells were stably transduced with retroviruses encoding GFP-tagged wild-type GTSE1, Tetra SA (phospho-deficient), or Tetra SD (phospho-mimic). Subsequent CHX chase experiments showed a slower degradation kinetics of the Tetra SD mutant compared to the Tetra SA mutant and wild-type GTSE1 (**Figure 3E,F**). These stable cell lines, expressing fluorescent GTSE1 variants, were further analyzed via time-lapse microscopy during a CHX chase

to quantify protein degradation through the diminishing fluorescence intensity at different times. The Tetra SD mutant exhibited a statistically significant slower fluorescence decrease rate than both Tetra SA and WT, indicating reduced degradation (**Figure 3G,H** [↗](#)).

Finally, we treated U2OS cells with CHX together with inhibitors targeting different degradation systems: MG132 (a proteasome inhibitor), MLN4924 (a CRL inhibitor), or Bafilomycin A (an autophagy inhibitor) (**Figure 3I** [↗](#)). The stabilization of GTSE1 in the presence of MG132 and MLN4924, but not Bafilomycin A, indicates that GTSE1 degradation mainly occurs via the ubiquitin-proteasome system (UPS), specifically implicating the involvement of a CRL. However, GTSE1 does not appear to be a substrate of CRL4<sup>AMBRA1</sup> [↗](#), as indicated by the lack of a physical interaction between AMBRA1 and GTSE1 (Figure supplement 3E).

Next, we delved into the potential implications of GTSE1 phosphorylation by the cyclin D1-CDK4 complex. Previous research has connected GTSE1 with fundamental cellular processes, such as cell proliferation [↗](#) and cell migration and invasion [↗](#). Leveraging data from CPTAC, we examined possible correlations between both GTSE1 protein levels (Figure supplement 4A) and levels of phosphorylated GTSE1 (**Figure 4A** [↗](#)) with markers of cell proliferation and cell migration across various cancer types. GTSE1 abundance and phosphorylation exhibited a statistically significant positive correlation with several proteins integral to cell proliferation, including PCNA, KI67, and MCM2, across multiple cancer cohorts. Conversely, in contrast to data suggesting a role for GTSE1 in promoting cell migration [↗](#), GTSE1 levels and phosphorylation demonstrated a negative trend with proteins associated with cell migration and epithelial-mesenchymal transition (EMT), such as Vimentin, MMP1, and ETS1, but these did not attain statistical significance.

To explore the influence of cyclin D1-mediated phosphorylation of GTSE1 on cellular phenotypes, we assessed the proliferation potential of AMBRA1 knockout cells relative to their parental counterparts. AMBRA1 KO cells displayed an enhanced proliferation rate (Figure supplement 4B), in agreement with the literature [↗](#). We then conducted comparable growth analyses using U2OS cells stably expressing various GTSE1 constructs. Cells stably expressing the Tetra SD mutant exhibited a higher proliferation rate compared to cells expressing either Tetra SA or WT GTSE1 (**Figure 4B** [↗](#)). Moreover, evaluations of cellular proliferation conducted using Cell Trace dye demonstrated that cells harboring the Tetra-SD mutant displayed an elevated proliferative index (**Figure 4C** [↗](#)). This was evidenced by a greater number of cell generations and smaller fraction of non-divided cells relative to cells expressing WT GTSE1. Moreover, the increase in proliferation was much more evident in the Tetra-SD compared to the Tetra-SA mutant (**Figure 4C** [↗](#)).

Cyclin D1 overexpression is a hallmark of many cancers, where it facilitates oncogenic transformation and progression. Amplifications and overexpression of the *CCND1* gene are seen in a diverse array of cancers, with amplifications in up to 15% to 20% of breast cancers and overexpression in over 50% of mantle cell lymphomas [↗](#). The pervasiveness of cyclin D1 dysregulation in cancer highlights the critical need to understand its downstream effects. Despite this, the full spectrum of substrates and their impact on cellular function and oncogenesis remain poorly explored [↗](#). In the present study, we identified GTSE1, a pro-proliferative protein, as a novel substrate of the cyclin D1-CDK4 complex. Our data indicate that cyclin D1-CDK4 is responsible for the phosphorylation of GTSE1 on four residues (S91, S262, S454, and S724). In contrast, cyclin A2-CDK2, cyclin E1-CDK2, and cyclin B1-CDK1 target additional and/or different sites as shown by the fact that they still induced mobility shift of the “Tetra SA” mutant in cultured cells. GTSE1 has been established as a substrate of G2 and M cyclins [↗](#), but we observed that in human cells, when D-type cyclins are stabilized in the absence of AMBRA1, GTSE1 becomes phosphorylated also in G1. Accordingly, overexpression of cyclin D1-CDK4 induce GTSE1 phosphorylation. Thus, we propose that GTSE1 is phosphorylated by CDK4 and CDK6 particularly in pathological states, such as cancers displaying overexpression of D-type cyclins. In turn, GTSE1 phosphorylation induces its stabilization, leading to increased levels that contribute to enhanced

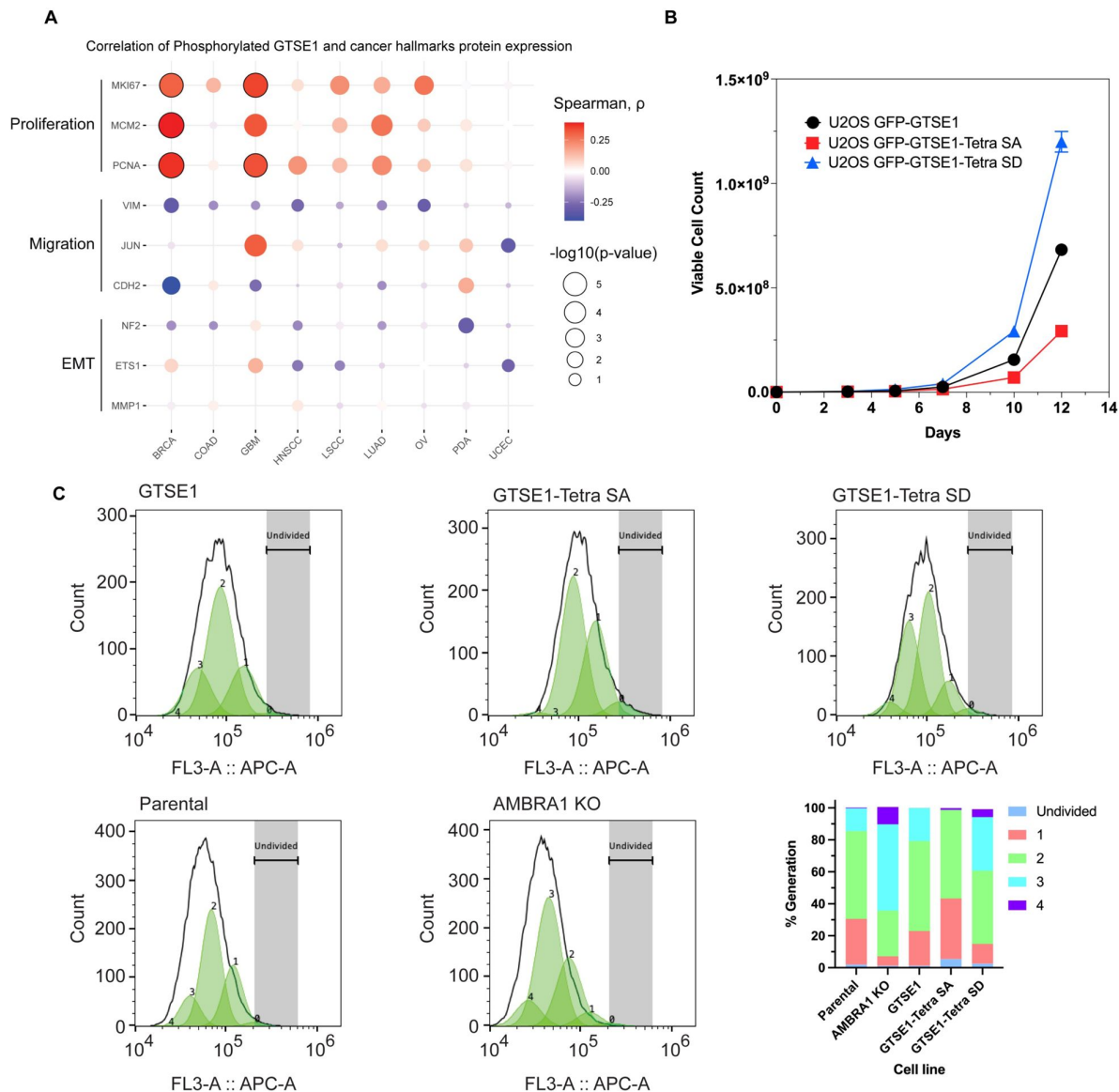


**Figure 4**

### Increased cell proliferation upon cyclin D1-CDK4-mediated phosphorylation and stabilization of GTSE1

A) Bubble plot derived from CPTAC data analysis showing the correlation between the abundance of the bulk phosphopeptides of GTSE1 and the levels of proteins involved in cell proliferation or cell migration across various cancer types. The color intensity of each bubble represents the Spearman correlation coefficient, while the bubble size indicates the negative log<sub>10</sub> transformation of the p-values. Bubbles outlined in black indicate statistically significant correlations with  $q\text{-value} < 0.0001$ , adjusted by Benjamini-Hochberg (BH) method.

B) Growth curve analysis comparing the proliferation of U2OS cells stably expressing GFP-tagged wild-type GTSE1, GTSE1 Tetra SA (phospho-deficient), or GTSE1 Tetra SD (phospho-mimetic). A  $p\text{-value} < 0.05$  was considered significant ( $n=3$  per cell line)

C) Proliferation analysis using CellTrace™ Far Red dye to assess the division of U2OS cells expressing wild-type GTSE1, Tetra SA, and Tetra SD, alongside a comparison between parental and AMBRA1 KO U2OS cells. Following staining, the dye dilutes progressively with each cell division, allowing for the distinction of successive generations by the relative decrease in fluorescence intensity. Fluorescence-activated cell sorting was employed to accurately measure the dye dilution and thereby quantify the discrete populations representing each generation of the cell line. The gating strategy was implemented to identify live, single cells positive for GFP, as detailed in Figure supplement 4C. The percentages of cells in each generation, indicative of proliferative capacity, are displayed graphically on the right lower panel.

cell proliferation. It is also possible that GTSE1 is also recognized in specific cell types and in particular stage/s of embryogenesis, when cyclin D1 levels are elevated, and high cell proliferation is crucial for proper tissue formation<sup>35</sup>. The prolonged half-life of GTSE1 consequent to cyclin D1-CDK4-mediated phosphorylation suggests a mechanism through which cells could modulate the abundance of a key regulatory protein without necessitating new protein synthesis. This post-translational regulation could be a critical determinant in the rapid response to mitogenic signals or environmental cues.

Our study further established a correlation between phosphorylation of GTSE1 and markers of cell proliferation, as well as poor prognosis in human cancers, providing a partial explanatory basis for the proliferative phenotype associated with elevated D-type cyclins observed in human tumors. Future studies are warranted to further dissect the molecular mechanisms underpinning GTSE1's function in cell cycle regulation and its contribution to the cancerous phenotype, potentially paving the way for novel cancer therapeutics.

## Materials and Methods

### Cell Culture and Transduction

HEK293T, HCT116, T98G and U2OS cell lines were cultured under specific conditions suited to each cell type. HEK293T and T98G cells were cultured in DMEM (Dulbecco's Modified Eagle Medium), while HCT116 and U2OS cells were maintained in McCoy's 5A medium. All media were supplemented with 10% fetal bovine serum (FBS) and 1% penicillin-streptomycin and cells were incubated at 37°C in a humidified atmosphere containing 5% CO<sub>2</sub>.

For retroviral production, HEK293T cells were co-transfected with GTSE1 expression constructs along with VSVG and PAX packaging plasmids using Lipofectamine 3000 (Invitrogen) according to the manufacturer's instructions. Virus-containing supernatants were harvested 48 hours post-transfection, filtered through a 0.45 µm pore size filter, and used for transducing target HCT116 and U2OS cells in the presence of 8 µg/ml Polybrene. Stably transduced cells were selected by sorting for EGFP positive cells by cell sorter.

For transient transfection studies, HEK293T cells were transfected with various plasmids using PEI (Polysciences); HCT-116 and U-2 OS were transiently transfected with Lipofectamine 3000 (Thermo Fisher Scientific). Where indicated, 24 h after transfection, cells were treated with MG132 or MLN4924 for 4 h before collection, following a protocol optimized for maximal transfection efficiency and minimal cellular toxicity. Post-transfection, cells were maintained under standard culture conditions before being harvested for subsequent experiments.

### Plasmids

Homo sapiens cDNAs were amplified by PCR using KAPA HiFi DNA Polymerase (Kapa Biosystems) and sub-cloned into a variety of vector backbones, including modified pCDNA3.1 vectors containing N-terminal Flag or HA and pBABE-PURO retroviral vectors containing N-terminal eGFP. FFSS indicates a tandem 2×Flag–2×Strep tag. Site-directed mutagenesis was performed using KAPA HiFi DNA Polymerase (Kapa Biosystems).

### Western Blotting and antibodies

Protein extracts were prepared using RIPA buffer supplemented with protease inhibitors (Complete ULTRA, Roche) and phosphatase inhibitors (PhosSTOP, Roche). The insoluble fraction was removed by centrifugation (20,000g) for 15 min at 411°C. Protein concentrations in cell lysates were normalized using the Pierce BCA Protein Assay Kit (Thermo Fisher Scientific), according to the manufacturer's instructions. Proteins were separated by SDS-PAGE and transferred to PVDF

membranes. Membranes were blocked with 5% non-fat dry milk and incubated with primary antibodies overnight at 4°C, followed by HRP-conjugated secondary antibodies. Enhanced chemiluminescence (ECL, Thermo Fisher Scientific) was used for detection. Protein separation by Phos-tag gels was performed using self-cast gels. For the analysis of GTSE1, gels were composed of 6% acrylamide, whereas 7.5% acrylamide gels were utilized for the C-terminal region of Retinoblastoma. Both gels were supplemented with 40  $\mu\text{M}$   $\text{Zn}^{+2}$ -Phos-tag (Fujifilm Wako Chemicals U.S.A.) to achieve high-resolution separation of phosphorylated protein species. The separation protocol was conducted according to the manufacturer's instructions. The following antibodies were used: GTSE1 (1:1000, Bethyl Laboratories #A302-274A),  $\beta$ -actin (1:5,000, Sigma-Aldrich A5441), AMBRA1 (1:1,000, Proteintech Group 13762-1-AP), cyclin A (1:5,000, M.P. laboratory), cyclin B1 (1:5,000, M.P. laboratory), cyclin D1 (1:1,000, Abcam ab16663), p-cyclin D1 (T286) (1:1,000, Cell Signaling Technology 3300S), cyclin E (1:1,000, Santa Cruz Biotechnology sc-247), Flag (1:2,000, Sigma-Aldrich F1804), Flag (1:2,000, Sigma-Aldrich F7425), GST (1:5,000, GE Healthcare 27457701), HA (1:2,000, Bethyl Laboratories A190-108A), LC-3 (1:5,000, Novus Biological NB100-2220), p21 (1:1,000, Cell Signaling Technology 2947S), p27 (1:1,000, BD Biosciences 610241), p62 (1:5,000, MBL International PM045), RB (1:1,000, Cell Signaling Technology 9313S), RB (1:1,000, Cell Signaling Technology 9309S), p-RB (S807/811) (1:1,000, Cell Signaling Technology 9308S), SKP1 (1:5,000, M.P. laboratory),  $\alpha$ -tubulin (1:5,000, Sigma-Aldrich T6074). A phospho-specific antibody against GTSE1 phosphorylated on Ser262 was generated by YenZym. Briefly, a peptide containing the phospho-epitope, which includes amino acids 254-269 (KPKKEIPApSPSRTKIP) was synthesized. This peptide was then used to immunize rabbits, using Cys-KLH as immunogen, prompting the production of antibodies against the phospho-epitope. Following immunization, phospho-specific antibodies were purified by utilizing a phosphorylated peptide conjugated affinity matrix. To ensure the specificity and efficacy of the antibody, an ELISA was performed on both pre- and post-purified serum.

## In vitro phosphorylation

Assays were carried out using 1 microgram of recombinant substrate proteins in the presence or absence of 0.1 microgram of kinase enzymes. Where indicated, 1  $\mu\text{M}$  Palbociclib was added to reaction mixtures containing CDK4 and Cyclin D1 and subjected to pre-incubation on ice for 10 minutes before the addition of the recombinant substrates. The phosphorylation reaction was conducted in kinase reaction buffer, containing 25 mM Tris-HCl (pH 7.5), 5 mM beta-glycerophosphate, 2 mM dithiothreitol (DTT), 0.1 mM  $\text{Na}_3\text{VO}_4$ , 10 mM  $\text{MgCl}_2$ , and 2 mM ATP. The reaction mixture was maintained at 30°C for a duration of 1 hour. To terminate the reaction, Laemmli buffer containing SDS and beta-mercaptoethanol was added to the samples, followed by heating at 95°C for 10 minutes.

## Chemicals and Reagents

Cycloheximide, Bafilomycin A1, MG132, and MLN4924 were obtained from Sigma-Aldrich (United States). PF-06873600 and Palbociclib were purchased from Selleckchem (United States). RO-3306 was acquired from Roche (United States). Auxin (Indole-3-acetic acid) and Doxycycline were sourced from Thermo Fisher Scientific (United States). Rb (Retinoblastoma Human Recombinant) fused with a 6X His tag, containing the C-terminal 792-928 aa, was obtained from Raybiotech (United States). GTSE1, full-length, with N-terminal GST and C-terminal HIS tag, was sourced from Origene (United States). GST-tagged ERK2 was acquired from Abcam (United States). His-tagged Human Cyclin D1 and CDK4 were obtained from LSBio (United States).

## Growth Curve Analysis

Cell proliferation was assessed by plating cells at a fixed density and counting at specific intervals using Vi-CELL BLU Cell Viability Analyzer (Beckman Coulter). For cell count normalization, Trypan Blue exclusion was used to assess cell viability.

## Cell Proliferation Analysis

Cells were labeled with the CellTrace™ Far Red dye (Invitrogen) according to the manufacturer's instructions, ensuring that the initial fluorescence intensity was homogenous across the cell population. This method relies on the principle of dye dilution to trace multiple generations of cells through flow cytometry. Following labeling, the cells were cultured under appropriate conditions to allow for cell division (confluency < 70%). Following five generation time, samples were collected and subjected to flow cytometric analysis. The progressive halving of the fluorescent dye intensity, as a result of cell division, was monitored, enabling the quantification of cell generations.

## Cell Cycle Studies

T98G cells were synchronized by serum starvation. Subconfluent plates of cells were trypsinized washed with PBS, and replated in DMEM containing 0.01% FBS. Cells were kept in this medium for 72 hours before they were trypsinized and replated at 70% confluency in DMEM containing 10% FBS to allow for cell cycle re-entry. Cells were collected at various time points following serum re-addition by scraping.

## Time Lapse Fluorescence Monitoring

For the monitoring of GFP-tagged GTSE1 degradation, U2OS cells were plated at a density of 50,000 cells per well within 96-well plates. Following a period of 24 hours from plating, the cells were subjected to live cell imaging using the Cytation 5 Cell Imaging Reader (BioTek, Winooski, VT), which is equipped with a dedicated module for real-time cell analysis. The imaging apparatus maintained the cells in an optimal environment, regulated at 37°C with 5% CO<sub>2</sub> levels. A Far Red cell tracer dye was applied to the cells prior to imaging, providing a distinct cellular outline for accurate identification during subsequent analysis. Images were captured at predetermined intervals following treatment with cycloheximide (CHX). Fluorescent emissions from both EGFP and Far Red spectra were monitored. Post-acquisition, images were analyzed to measure the cumulative EGFP fluorescent intensity within the confines delineated by the Far Red cellular demarcation. All procedures were conducted in triplicates.

## Bioinformatic Analysis

Bioinformatic analysis was performed using R statistical packages. For the visualization of tables, the 'formattable' package in R was employed. Differential proteomic profiling comparing parental U2OS cells to AMBRA1 knockout (KO) U2OS cells, utilized raw data from a shotgun proteomic screen previously published<sup>11</sup>[\[11\]](#). Proteins differentially expressed with an adjusted p-value < 0.05 were ordered according to the log<sub>2</sub> fold change (Log<sub>2</sub>FC) comparing AMBRA1 KO to parental cells. The significance of the differentially expressed proteins was determined by the False Discovery Rate (FDR) method. An annotated list of phosphorylated proteins that contain the canonical CDK phosphorylation site [S/T\*]PX[K/R] utilized the PhosphoSitePlus database<sup>23</sup>[\[23\]](#). This list was integrated with the proteomic data from the prior screen by matching gene names, to identify potential CDK substrates altered in the AMBRA1 KO context. The bioinformatic analysis for assessing the differential abundance and phosphorylation levels of GTSE1, as well as the correlation of GTSE1 abundance with different protein signatures in various cancer cohorts was conducted utilizing data from the Clinical Proteomic Tumor Analysis Consortium (CPTAC) database<sup>36</sup>[\[36\]](#).

## Acknowledgements

We thank Dr. Gregory David for critically reading the manuscript. MP is thankful to TM Thor and TB Balduur for their continuous support. This work was supported by NIH GM136250 to MP. MP is an investigator with the Howard Hughes Medical Institute. SK is a recipient of the Life Sciences Research Foundation (LSRF) Postdoctoral Fellowship and has been an EMBO Long Term Postdoctoral Fellow. NGV and TJGR are thankful for NIH Institutional Training Grant (T32GM136542). TJGR and KVR thank HHMI for Gilliam Fellowship (GT15758) support.

## Author contributions

MP conceived, supervised, and coordinated the study. SK supervised and coordinated the study. NGV, DS, GR, and SK designed, carried out the experiments, and analyzed the data. For some experiments, they were helped by EL, MK, D Spasskaia and QZ. MP, TJGR and KVR performed the CPTAC related analyses. SK, NGV, and MP wrote the paper with input from all authors.

## Declaration of interests

MP is or has been an advisor for and has financial interests in SEED Therapeutics, Triana Biomedicines, and CullGen, Kymera Therapeutics, and Umbra Therapeutics. The other authors have no competing interests to declare.

## References

- 1 Musgrove E. A., Caldon C. E., Barraclough J., Stone A., Sutherland R. L. (2011) **Cyclin D as a therapeutic target in cancer** *Nat Rev Cancer* **11**:558–572 <https://doi.org/10.1038/nrc3090>
- 2 Fassl A., Geng Y., Sicinski P. (2022) **CDK4 and CDK6 kinases: From basic science to cancer therapy** *Science* **375** <https://doi.org/10.1126/science.abc1495>
- 3 Alvarez-Fernandez M., Malumbres M. (2020) **Mechanisms of Sensitivity and Resistance to CDK4/6 Inhibition** *Cancer Cell* **37**:514–529 <https://doi.org/10.1016/j.ccell.2020.03.010>
- 4 Behan F. M., et al. (2019) **Prioritization of cancer therapeutic targets using CRISPR-Cas9 screens** *Nature* **568**:511–516 <https://doi.org/10.1038/s41586-019-1103-9>
- 5 Beroukhi R., et al. (2010) **The landscape of somatic copy-number alteration across human cancers** *Nature* **463**:899–905 <https://doi.org/10.1038/nature08822>
- 6 Curtin J. A., et al. (2005) **Distinct sets of genetic alterations in melanoma** *N Engl J Med* **353**:2135–2147 <https://doi.org/10.1056/NEJMoa050092>
- 7 Bignell G. R., et al. (2010) **Signatures of mutation and selection in the cancer genome** *Nature* **463**:893–898 <https://doi.org/10.1038/nature08768>
- 8 Parsons D. W., et al. (2008) **An integrated genomic analysis of human glioblastoma multiforme** *Science* **321**:1807–1812 <https://doi.org/10.1126/science.1164382>
- 9 Jones S., et al. (2008) **Core signaling pathways in human pancreatic cancers revealed by global genomic analyses** *Science* **321**:1801–1806 <https://doi.org/10.1126/science.1164368>
- 10 Simoneschi D., et al. (2021) **CRL4(AMBRA1) is a master regulator of D-type cyclins** *Nature* <https://doi.org/10.1038/s41586-021-03445-y>
- 11 Chaikovsky A. C., et al. (2021) **The AMBRA1 E3 ligase adaptor regulates the stability of cyclin D** *Nature* **592**:794–798 <https://doi.org/10.1038/s41586-021-03474-7>
- 12 Martinez-Jimenez F., et al. (2020) **A compendium of mutational cancer driver genes** *Nat Rev Cancer* **20**:555–572 <https://doi.org/10.1038/s41568-020-0290-x>
- 13 Kastan M. B., Bartek J. (2004) **Cell-cycle checkpoints and cancer** *Nature* **432**:316–323 <https://doi.org/10.1038/nature03097>
- 14 Liu X. S., Li H., Song B., Liu X. (2010) **Polo-like kinase 1 phosphorylation of G2 and S-phase-expressed 1 protein is essential for p53 inactivation during G2 checkpoint recovery** *EMBO Rep* **11**:626–632 <https://doi.org/10.1038/embor.2010.90>
- 15 Bublik D. R., Scolz M., Triolo G., Monte M., Schneider C. (2010) **Human GTSE-1 regulates p21(CIP1/WAF1) stability conferring resistance to paclitaxel treatment** *J Biol Chem* **285**:5274–5281 <https://doi.org/10.1074/jbc.M109.045948>

- 16 Monte M., et al. (2003) **The cell cycle-regulated protein human GTSE-1 controls DNA damage-induced apoptosis by affecting p53 function** *J Biol Chem* **278**:30356–30364 <https://doi.org/10.1074/jbc.M302902200>
- 17 Monte M., et al. (2004) **hGTSE-1 expression stimulates cytoplasmic localization of p53** *J Biol Chem* **279**:11744–11752 <https://doi.org/10.1074/jbc.M311123200>
- 18 Collavin L., Monte M., Verardo R., Pflieger C., Schneider C. (2000) **Cell-cycle regulation of the p53-inducible gene B99** *FEBS Lett* **481**:57–62 [https://doi.org/10.1016/s0014-5793\(00\)01969-4](https://doi.org/10.1016/s0014-5793(00)01969-4)
- 19 Bendre S., et al. (2016) **GTSE1 tunes microtubule stability for chromosome alignment and segregation by inhibiting the microtubule depolymerase MCAK** *J Cell Biol* **215**:631–647 <https://doi.org/10.1083/jcb.201606081>
- 20 Scolz M., et al. (2012) **GTSE1 is a microtubule plus-end tracking protein that regulates EB1-dependent cell migration** *PLoS One* **7** <https://doi.org/10.1371/journal.pone.0051259>
- 21 Singh D., Schmidt N., Muller F., Bange T., Bird A. W. (2021) **Destabilization of Long Astral Microtubules via Cdk1-Dependent Removal of GTSE1 from Their Plus Ends Facilitates Prometaphase Spindle Orientation** *Curr Biol* **31**:766–781 <https://doi.org/10.1016/j.cub.2020.11.040>
- 22 Monte M., et al. (2000) **Cloning, chromosome mapping and functional characterization of a human homologue of murine gtse-1 (B99) gene** *Gene* **254**:229–236 [https://doi.org/10.1016/s0378-1119\(00\)00260-2](https://doi.org/10.1016/s0378-1119(00)00260-2)
- 23 Hornbeck P. V., et al. (2015) **PhosphoSitePlus, 2014: mutations, PTMs and recalibrations** *Nucleic Acids Res* **43**:D512–520 <https://doi.org/10.1093/nar/gku1267>
- 24 Tan K., et al. (2023) **Pan-cancer analyses reveal GTSE1 as a biomarker for the immunosuppressive tumor microenvironment** *Medicine (Baltimore)* **102** <https://doi.org/10.1097/MD.00000000000034996>
- 25 Lin F., et al. (2019) **GTSE1 is involved in breast cancer progression in p53 mutation-dependent manner** *J Exp Clin Cancer Res* **38** <https://doi.org/10.1186/s13046-019-1157-4>
- 26 Lei P., Zhang M., Li Y., Wang Z. (2023) **High GTSE1 expression promotes cell proliferation, metastasis and cisplatin resistance in ccRCC and is associated with immune infiltrates and poor prognosis** *Front Genet* **14** <https://doi.org/10.3389/fgene.2023.996362>
- 27 Kaulich M., et al. (2021) **A Cdk4/6-dependent phosphorylation gradient regulates the early to late G1 phase transition** *Sci Rep* **11** <https://doi.org/10.1038/s41598-021-94200-w>
- 28 Yesbolatova A., et al. (2020) **The auxin-inducible degron 2 technology provides sharp degradation control in yeast, mammalian cells, and mice** *Nat Commun* **11** <https://doi.org/10.1038/s41467-020-19532-z>
- 29 Lai W., et al. (2021) **GTSE1 promotes prostate cancer cell proliferation via the SP1/FOXM1 signaling pathway** *Lab Invest* **101**:554–563 <https://doi.org/10.1038/s41374-020-00510-4>
- 30 Wu X., et al. (2017) **GTSE1 promotes cell migration and invasion by regulating EMT in hepatocellular carcinoma and is associated with poor prognosis** *Sci Rep* **7** <https://doi.org/10.1038/s41598-017-05311-2>

- 31 Li S. S., et al. (2021) **GTSE1 promotes SNAIL1 degradation by facilitating its nuclear export in hepatocellular carcinoma cells** *Mol Med Rep* **23** <https://doi.org/10.3892/mmr.2021.12093>
- 32 Cancer Genome Atlas Research, N. (2012) **Comprehensive genomic characterization of squamous cell lung cancers** *Nature* **489**:519–525 <https://doi.org/10.1038/nature11404>
- 33 Sherr C. J. (2000) **Cell cycle control and cancer** *Harvey Lect* **96**:73–92
- 34 Knudsen E. S., Knudsen K. E. (2008) **Tailoring to RB: tumour suppressor status and therapeutic response** *Nat Rev Cancer* **8**:714–724 <https://doi.org/10.1038/nrc2401>
- 35 Ter Huurne M., Stunnenberg H. G. (2021) **G1-phase progression in pluripotent stem cells** *Cell Mol Life Sci* **78**:4507–4519 <https://doi.org/10.1007/s00018-021-03797-8>
- 36 Ellis M. J., et al. (2013) **Connecting genomic alterations to cancer biology with proteomics: the NCI Clinical Proteomic Tumor Analysis Consortium** *Cancer Discov* **3**:1108–1112 <https://doi.org/10.1158/2159-8290.CD-13-0219>
- 37 Cancer Genome Atlas Research, N., et al. (2013) **The Cancer Genome Atlas Pan-Cancer analysis project** *Nat Genet* **45**:1113–1120 <https://doi.org/10.1038/ng.2764>
- 38 Tang Z., Kang B., Li C., Chen T., Zhang Z. (2019) **GEPIA2: an enhanced web server for large-scale expression profiling and interactive analysis** *Nucleic Acids Res* **47**:W556–W560 <https://doi.org/10.1093/nar/gkz430>
- 39 Varadarajan A. R., et al. (2020) **A Proteogenomic Resource Enabling Integrated Analysis of Listeria Genotype-Proteotype-Phenotype Relationships** *J Proteome Res* **19**:1647–1662 <https://doi.org/10.1021/acs.jproteome.9b00842>

## Editors

Reviewing Editor

**Ivan Topisirovic**

Jewish General Hospital, Montreal, Canada

Senior Editor

**Jonathan Cooper**

Fred Hutchinson Cancer Research Center, Seattle, United States of America

## Reviewer #1 (Public review):

Summary:

García-Vázquez et al. identify GTSE1 as a novel target of the cyclin D1-CDK4/6 kinases. The authors show that GTSE1 is phosphorylated at four distinct serine residues and that this phosphorylation stabilizes GTSE1 protein levels to promote proliferation.

Strengths:

The authors support their findings with several previously published results, including databases. In addition, the authors perform a wide range of experiments to support their findings.

#### Weaknesses:

I feel that important controls and considerations in the context of the cell cycle are missing. Cyclin D1 overexpression, Palbociclib treatment and apparently also AMBRA1 depletion can lead to major changes in cell cycle distribution, which could strongly influence many of the observed effects on the cell cycle protein GTSE1. It is therefore important that the authors assess such changes and normalize their results accordingly.

<https://doi.org/10.7554/eLife.101075.1.sa3>

#### Reviewer #2 (Public review):

##### Summary:

The manuscript by García-Vázquez et al identifies the G2 and S phases expressed protein 1(GTSE1) as a substrate of the CycD-CDK4/6 complex. CycD-CDK4/6 is a key regulator of the G1/S cell cycle restriction point, which commits cells to enter a new cell cycle. This kinase is also an important therapeutic cancer target by approved drugs including Palbociclib. Identification of substrates of CycD-CDK4/6 can therefore provide insights into cell cycle regulation and the mechanism of action of cancer therapeutics. A previous study identified GTSE1 as a target of CycB-Cdk1 but this appears to be the first study to address the phosphorylation of the protein by Cdk4/6.

The authors identified GTSE1 by mining an existing proteomic dataset that is elevated in AMBRA1 knockout cells. The AMBRA1 complex normally targets D cyclins for degradation. From this list, they then identified proteins that contain a CDK4/6 consensus phosphorylation site and were responsive to treatment with Palbociclib.

The authors show CycD-CDK4/6 overexpression induces a shift in GTSE1 on phostag gels that can be reversed by Palbociclib. In vitro kinase assays also showed phosphorylation by CDK4. The phosphorylation sites were then identified by mutagenizing the predicted sites and phostag got to see which eliminated the shift.

The authors go on to show that phosphorylation of GTSE1 affects the steady state level of the protein. Moreover, they show that expression and phosphorylation of GTSE1 confer a growth advantage on tumor cells and correlate with poor prognosis in patients.

##### Strengths:

The biochemical and mutagenesis evidence presented convincingly show that the GTSE1 protein is indeed a target of the CycD-CDK4 kinase. The follow-up experiments begin to show that the phosphorylation state of the protein affects function and has an impact on patient outcomes.

#### Weaknesses:

It is not clear at which stage in the cell cycle GTSE1 is being phosphorylated and how this is affecting the cell cycle. Considering that the protein is also phosphorylated during mitosis by CycB-Cdk1, it is unclear which phosphorylation events may be regulating the protein.

<https://doi.org/10.7554/eLife.101075.1.sa2>

#### Reviewer #3 (Public review):

##### Summary:

This paper identifies GTSE1 as a potential substrate of cyclin D1-CDK4/6 and shows that GTSE1 correlates with cancer prognosis, probably through an effect on cell proliferation. The main problem is that the phosphorylation analysis relies on the over-expression of cyclin D1. It is unclear if the endogenous cyclin D1 is responsible for any phosphorylation of GTSE1 in vivo, and what, if anything, this moderate amount of GTSE1 phosphorylation does to drive proliferation.

**Strengths:**

There are few bonafide cyclin D1-Cdk4/6 substrates identified to be important in vivo so GTSE1 represents a potentially important finding for the field. Currently, the only cyclin D1 substrates involved in proliferation are the Rb family proteins.

**Weaknesses:**

The main weakness is that it is unclear if the endogenous cyclin D1 is responsible for phosphorylating GTSE1 in the G1 phase. For example, in Figure 2G there doesn't seem to be a higher band in the phos-tag gel in the early time points for the parental cells. This experiment could be redone with the addition of palbociclib to the parental to see if there is a reduction in GTSE1 phosphorylation and an increase in the amount in the G1 phase as predicted by the authors' model.

The experiments involving palbociclib do not disentangle cell cycle effects. Adding Cdk4 inhibitors will progressively arrest more and more cells in the G1 phase and so there will be a reduction not just in Cdk4 activity but also in Cdk2 and Cdk1 activity. More experiments, like the serum starvation/release in Figure 2G, with synchronized populations of cells would be needed to disentangle the cell cycle effects of palbociclib treatment.

It is unclear if GTSE1 drives the G1/S transition. Presumably, this is part of the authors' model and should be tested.

The proliferation assays need to be more quantitative. Figure 4B should be plotted on a log scale so that the slope can be used to infer the proliferation rate of an exponentially increasing population of cells. Figure 4c should be done with more replicates and error analysis since the effects shown in the lower right-hand panel are modest.

<https://doi.org/10.7554/eLife.101075.1.sa1>

**Author response:**

**Reviewer #1:**

*Summary:*

*García-Vázquez et al. identify GTSE1 as a novel target of the cyclin D1-CDK4/6 kinases. The authors show that GTSE1 is phosphorylated at four distinct serine residues and that this phosphorylation stabilizes GTSE1 protein levels to promote proliferation.*

*Strengths:*

*The authors support their Findings with several previously published results, including databases. In addition, the authors perform a wide range of experiments to support their Findings.*

*Weaknesses:*

*I feel that important controls and considerations in the context of the cell cycle are missing. Cyclin D1 overexpression, Palbociclib treatment and apparently also AMBRA1 depletion can lead to major changes in cell cycle distribution, which could strongly influence many of the observed effects on the cell cycle protein GTSE1. It is therefore important that the authors assess such changes and normalize their results accordingly.*

We have approached the question of GTSE1 phosphorylation to account for potential cell cycle effects from multiple angles:

(i) We conducted *in vitro* experiments with purified, recombinant proteins and shown that GTSE1 is phosphorylated by cyclin D1-CDK4 in a cell-free system (Figure 2A-C). This experiment provides direct evidence of GTSE1 phosphorylation by cyclin D1-CDK4 without the influence of any other cell cycle effectors.

(ii) We present data using synchronized AMBRA1 KO cells (Figure 2G and Supplementary Figure 3B). As shown previously (Simoneschi *et al.*, *Nature* 2021, PMC8875297), AMBRA1 KO cells progress faster in the cell cycle but they are still synchronized as shown, for example by the mitotic phosphorylation of Histone H3. Under these conditions we observed that while phosphorylation of GTSE1 in parental cells peaks at the G2/M transition, AMBRA1 KO cells exhibited sustained phosphorylation of GTSE1 across all cell cycle phases. This is evident when using Phos-tag gels as in the current top panel of Figure 2G. We now re-run one the biological triplicates of the synchronized cells using higher concentration of Zn<sup>2+</sup>-Phos-tag reagent and lower voltage to allow better separation. Under these conditions, GTSE1 phosphorylation is more apparent. In the new version of the paper, we will either show both blots or substitute the old panel with the new one. This experiment provides evidence that high levels of cyclin D1 in AMBRA1 KO cells affect GTSE1 independently of the specific points in the cell cycle.

(iii) The relative short half-life of GTSE1 (<4 hours) makes its levels sensitive to acute treatments such as Palbociclib or AMBRA1 depletion. The effects of these treatments on GTSE1 levels are measurable within a time frame too short to affect cell cycle progression in a meaningful way. For example, we used cells with fusion of endogenous AMBRA1 to a mini-Auxin Inducible Degron (mAID) at the N-terminus. This system allows for rapid and inducible degradation of AMBRA1 upon addition of auxin, thereby minimizing compensatory cellular rewiring. Again, we observed an increase in GTSE1 levels upon acute ablation of AMBRA1 (*i.e.*, in 8 hours) (Figure 3B), when no significant effects on cell cycle distribution are observed (please see Simoneschi *et al.*, *Nature* 2021, PMC8875297 and Rona *et al.*, *Mol. Cell* 2024, PMC10997477).

All together, these lines of evidence support our conclusion that GTSE1 is a target of cyclin D1-CDK4, independent of cell cycle effects. In conclusion, as stated in the Discussion section, GTSE1 has been established as a substrate of mitotic cyclins, but we observed that overexpression of cyclin D1-CDK4 induce GTSE1 phosphorylation at any point of the cell cycle. Thus, we propose that GTSE1 is phosphorylated by CDK4 and CDK6 particularly in pathological states, such as cancers displaying overexpression of D-type cyclins beyond the G1 phase. In turn, GTSE1 phosphorylation induces its stabilization, leading to increased levels that, as expected based on the existing literature, contribute to enhanced cell proliferation. So, the cyclin D1-CDK4/6 kinase-dependent phosphorylation of GTSE1 induces its stabilization independently of the cell cycle.

#### **Reviewer #2:**

##### *Summary:*

*The manuscript by García-Vázquez et al identifies the G2 and S phases expressed protein*

*1(GTSE1) as a substrate of the CycD-CDK4/6 complex. CycD-CDK4/6 is a key regulator of the G1/S cell cycle restriction point, which commits cells to enter a new cell cycle. This kinase is also an important therapeutic cancer target by approved drugs including Palbocyclib. Identification of substrates of CycD-CDK4/6 can therefore provide insights into cell cycle regulation and the mechanism of action of cancer therapeutics. A previous study identified GTSE1 as a target of CycB-Cdk1 but this appears to be the first study to address the phosphorylation of the protein by Cdk4/6.*

*The authors identified GTSE1 by mining an existing proteomic dataset that is elevated in AMBRA1 knockout cells. The AMBRA1 complex normally targets D cyclins for degradation. From this list, they then identified proteins that contain a CDK4/6 consensus phosphorylation site and were responsive to treatment with Palbocyclib.*

*The authors show CycD-CDK4/6 overexpression induces a shift in GTSE1 on phostag gels that can be reversed by Palbocyclib. In vitro kinase assays also showed phosphorylation by CDK4. The phosphorylation sites were then identified by mutagenizing the predicted sites and phostag got to see which eliminated the shift.*

*The authors go on to show that phosphorylation of GTSE1 affects the steady state level of the protein. Moreover, they show that expression and phosphorylation of GTSE1 confer a growth advantage on tumor cells and correlate with poor prognosis in patients.*

#### *Strengths:*

*The biochemical and mutagenesis evidence presented convincingly show that the GTSE1 protein is indeed a target of the CycD-CDK4 kinase. The follow-up experiments begin to show that the phosphorylation state of the protein affects function and has an impact on patient outcomes.*

#### *Weaknesses:*

*It is not clear at which stage in the cell cycle GTSE1 is being phosphorylated and how this is affecting the cell cycle. Considering that the protein is also phosphorylated during mitosis by CycB-Cdk1, it is unclear which phosphorylation events may be regulating the protein.*

In cells that do not overexpress cyclin D1, GTSE1 is phosphorylated at the G2/M transition, consistent with the known cyclin B1-CDK1-mediated phosphorylation of this protein. However, AMBRA1 KO cells exhibited high levels of cyclin D1 throughout the cell cycle and sustained phosphorylation of GTSE1 across all cell cycle points (Figure 2G and Supplementary Figure 3B). Please see also answer to Reviewer #1. Moreover, we show that, compared to the amino acids phosphorylated by cyclin D1-CDK4, cyclin B1-CDK1 phosphorylates GTSE1 on either additional residues or different sites (Figure 2H). Finally, we show that expression of a phospho-mimicking GTSE1 mutant leads to accelerated growth and an increase in the cell proliferative index (Figure 4C). However, we have not evaluated how phosphorylation affects the cell cycle distribution. We will perform FACS analyses and include them in the new version.

#### **Reviewer #3:**

##### *Summary:*

*This paper identifies GTSE1 as a potential substrate of cyclin D1-CDK4/6 and shows that GTSE1 correlates with cancer prognosis, probably through an effect on cell proliferation. The main problem is that the phosphorylation analysis relies on the over-expression of cyclin D1. It is unclear if the endogenous cyclin D1 is responsible for any phosphorylation*

*of GTSE1 in vivo, and what, if anything, this moderate amount of GTSE1 phosphorylation does to drive proliferation.*

**Strengths:**

*There are few bonafide cyclin D1-Cdk4/6 substrates identified to be important in vivo so GTSE1 represents a potentially important finding for the field. Currently, the only cyclin D1 substrates involved in proliferation are the Rb family proteins.*

**Weaknesses:**

*The main weakness is that it is unclear if the endogenous cyclin D1 is responsible for phosphorylating GTSE1 in the G1 phase. For example, in Figure 2G there doesn't seem to be a higher band in the phos-tag gel in the early time points for the parental cells. This experiment could be redone with the addition of palbociclib to the parental to see if there is a reduction in GTSE1 phosphorylation and an increase in the amount in the G1 phase as predicted by the authors' model. The experiments involving palbociclib do not disentangle cell cycle effects. Adding Cdk4 inhibitors will progressively arrest more and more cells in the G1 phase and so there will be a reduction not just in Cdk4 activity but also in Cdk2 and Cdk1 activity. More experiments, like the serum starvation/release in Figure 2G, with synchronized populations of cells would be needed to disentangle the cell cycle effects of palbociclib treatment.*

In normal cells, GTSE1 is phosphorylated at the G2/M transition in a cyclin B1-CDK1dependent manner. During G1, when the levels of cyclin D1 peak, GTSE1 is not phosphorylated. This could be due to a higher affinity between GTSE1 and mitotic cyclins as compared to G1 cyclins or to a higher concentration of mitotic cyclins compared to G1 cyclins. We show that higher levels of cyclin D1 induce GTSE1 phosphorylation during interphase, but we do not rely only on the overexpression of exogenous cyclin D1. In fact, we observe similar effect when we deplete endogenous AMBRA1, resulting in the stabilization of endogenous cyclin D1. As mentioned in the Discussion section, we propose that GTSE1 is phosphorylated by CDK4 and CDK6 particularly in pathological states, such as cancers displaying overexpression of D-type cyclins (i.e., the overexpression appears to overcome the lower affinity of the cyclin D1-GTSE1 complex). In sum, our study suggests that overexpression of cyclin D1, which is often observed in cancers cells beyond the G1 phase, induces phosphorylation of GTSE1 at all points in the cell cycle displaying high levels of cyclin D1. Please see also response to Reviewer #1. Concerning the experiments involving palbociclib, we limited confounding effects on the cell cycle by treating cells with palbociclib for only 4-6 hours. Under these conditions, there is simply not enough time for the cells to arrest in G1.

*It is unclear if GTSE1 drives the G1/S transition. Presumably, this is part of the authors' model and should be tested.*

We are not claiming that GTSE1 drives the G1/S transition. GTSE1 is known to promote cell proliferation, but how it performs this task is not well understood. Our experiments indicate that, when overexpressed, cyclin D1 promotes GTSE1 phosphorylation and its consequent stabilization. In agreement with the literature, we show that higher levels of GTSE1 promote cell proliferation. To measure cell cycle distribution upon expressing various forms of GTSE1, we will now perform FACS analyses and include them in the new version.

*The proliferation assays need to be more quantitative. Figure 4B should be plotted on a log scale so that the slope can be used to infer the proliferation rate of an exponentially increasing population of cells. Figure 4c should be done with more replicates and error analysis since the effects shown in the lower right-hand panel are modest.*

In Figure 4B, we plotted data in a linear scale as done in the past (Donato et al. Nature Cell Biol. 2017, PMC5376241) to better represent the changes in total cell number overtime. The experiments in Figure 4C were performed in triplicate. Error analysis was not included for simplicity, given the complexity of the data. We will include the other two sets of experiments in the revised version. While the effects shown in the lower right-hand panel of Figure 4C are modest, they demonstrate the same trend as those observed in the AMBRA KO cells (Figure 4C and Simoneschi et al., Nature 2021, PMC8875297). It's important to note that this effect is achieved through the stable expression of a single phosphomimicking protein, whereas AMBRA KO cells exhibit changes in numerous cell cycle regulators.

We appreciate the constructive comments and suggestions made by the reviewers, and we believe that the resulting additions and changes will improve the clarity and message of our study.

<https://doi.org/10.7554/eLife.101075.1.sa0>